Analysis of Limited Coverage Effects on Areal-Density Measurements in Inertial Confinement Fusion Implosions

V. Gopalaswamy,[1,2] R. Betti,[1,2,3] P. B. Radha,[1] A. J. Crilly,[4] K. M. Woo,[1] A. Lees,[1,2] C. A. Thomas,[1]
I. V. Igumenshchev,[1] S. C. Miller,[1,2] J. P. Knauer,[1] C. Stoeckl,[1] C. J. Forrest,[1] O. M. Mannion,[1,3,5] Z. L. Mohamed,[1,3]
H. G. Rinderknecht,[1] and P. V. Heuer[1]

[1]Laboratory for Laser Energetics, University of Rochester
[2]Department of Mechanical Engineering, University of Rochester
[3]Department of Physics and Astronomy, University of Rochester
[4]Imperial College London
[5]Sandia National Laboratories

To assess the quality of an inertial confinement fusion (ICF) experiment, various performance metrics based on the Lawson triple product[1–8] have been devised. These performance metrics must exceed a critical number to provide net energy gain. In direct-drive ICF implosions at the Omega Laser Facility,[9] the performance metric of interest is the so-called no-alpha normalized Lawson parameter χ

$$\chi = \rho R^{0.6}\left(0.12\frac{Y_{16}}{M}\right)^{0.34}. \tag{1}$$

In an experiment, the areal density and yield can be diagnosed directly, while the stagnated DT mass can be estimated from simulations or from experimental data to infer χ. When χ is close to unity, alpha heating dominates the energetics of a hot spot, leading to ignition, which is a prerequisite for high-gain implosions. Due to the strong dependence of χ on the ρR, an accurate diagnosis is of critical importance. On OMEGA, an approach that synthesizes experiments and simulations[10–12] to create predictive models has led to dramatic increases in experimental performance, primarily through increases in neutron yield. References 10–12 present highly accurate predictive models for the neutron yield, but do not address the ρR—primarily because these models are not sufficiently accurate to drive experimental design. Achieving a comparable quality of predictive capability for ρR as exists for the yield is a necessary prerequisite for the predictive-model–driven campaign on OMEGA to optimize ρR since the effective "step-size" of an iterative scheme to improve the ρR is roughly bounded below by the prediction uncertainty.

One reason for the lack of predictive capability for ρR is that it is an inherently 3-D measurement with different diagnostics integrating over varying regions of the sphere relative to a fixed line of sight. A predictive model for the 1-D–equivalent ρR, which is what we are attempting to optimize in experiments, will have an uncertainty that is at least as large as this limited coverage error, which in turn sets the minimum step-size of the iterative scheme to improve the ρR in experiments.

To generate physically reasonable 3-D configurations for use in *IRIS*, the 3-D radiation-hydrodynamic simulation *ASTER*[13] is used. Three configurations are considered. In the first, the effect of illumination asymmetry arising from the beam geometry is considered. In the second and third configurations, the illumination resulting from a fixed beam size of $R_b = 330\ \mu$m is modulated with varying $\ell = 1$, $m = 0$ and $\ell = 2$, $m = 0$ perturbations, respectively, both aligned along the $+z$ axis. The detectors used are specified in Table I, and the detector permutations are specified in Table II. The MRS virtual detector simulates the action of the magnetic recoil spectrometer,[14] while the P7/H10 BS virtual detectors simulate the action of the neutron-time-of-flight (nTOF) backscatter measurement.[15] The P7/H10 FW virtual detectors simulate the action of a hypothetical forward scatter measurement

Table I: Detector configurations used in this work. See Table II for the permutations used. The P7 and H10 nTOF detectors are located at the center of P7 and H7 in the OMEGA target chamber, respectively. At the present time, the nTOF's are only capable of backscatter (BS) measurements. The forward scatter (FW) measurement on the nTOF's is under investigation.

Detector	θ_{det} (rad)	ϕ_{det} (rad)
P7 FW	2.03	2.83
P7 BS	2.03	2.83
H10 FW	1.35	2.83
H10 BS	1.35	5.27

Table II: Detector perumutations that are considered in this work. Note that the MRS + P7BS permutation is the one that is currently used in OMEGA experiments. Due to the unique details of each detector and experiment, it is possible that some measurements may be compromised on certain experiments.

Configuration	P7 FW	P7 BS	H10 FW	H10 BS	MRS FW
MRS Only					
MRS + P7BS					
MRS + H10BS					x
MRS + P7/H10BS		x			x
MRS + P7/H10BS + P7FW		x		x	x
MRS + P7/H10BS + H10FW	x	x		x	x
All	x	x	x	x	x

from the nTOF's that are under investigation on OMEGA. Note that the "MRS + P7BS" permutation represents the currently used permutation on OMEGA to assess the 1-D–equivalent ρR. For each simulation, each permutation of detectors is evaluated for each pair of (θ', ϕ'). The 1-D–equivalent ρR [that is, the areal density of a perturbed implosion that is appropriate to use in Eq. (1)], $\langle \rho R \rangle$, is calculated by a harmonic average over the observed ρL by virtual detectors that are distributed uniformly over the sphere, where the ρL of a particular virtual detector is the neutron-averaged path length integral of the density for all primary (i.e., not scattered) virtual particles binned in that virtual detector and is the best estimate of the "real" areal density that would be seen by that detector.

First, consider the highest ℓ-mode simulation case of the beam mode. At stagnation, the shell can be moderately to severely perturbed due to the driven mode.[12] However, ρR is inferred in experiments from integrals over the neutron spectrum, which corresponds (assuming a point source) to sampling over conical sections of the shell. Combined with the distributed source of a real hot spot, the inferred ρR from either the backscatter or forward-scatter measurement is found to be uniform over the sphere (although it may still be degraded with respect to 1-D), as seen in Fig. 1.

Next, consider the effect of the $\ell = 1$ mode. The strength of the mode is parametrized by the effective ion-temperature asymmetry $R_T = T_{\text{max}}/T_{\text{min}}$ it generates, and bin configurations belonging to similar R_T together to visualize the results. It is found that as the number of detectors used to infer an average ρR increases, the error in that inference decreases, although some detectors are more valuable than others (e.g., P10 backscatter is more valuable than P7 backscatter), as visualized in Fig. 2. This is due to the fixed positions of the diagnostics with respect to each other. With sufficient detectors, the error due to the mode 1 for high-performance–relevant implosions (i.e., $R_T \rightarrow 1$) approaches the acceptable limit of 5%.

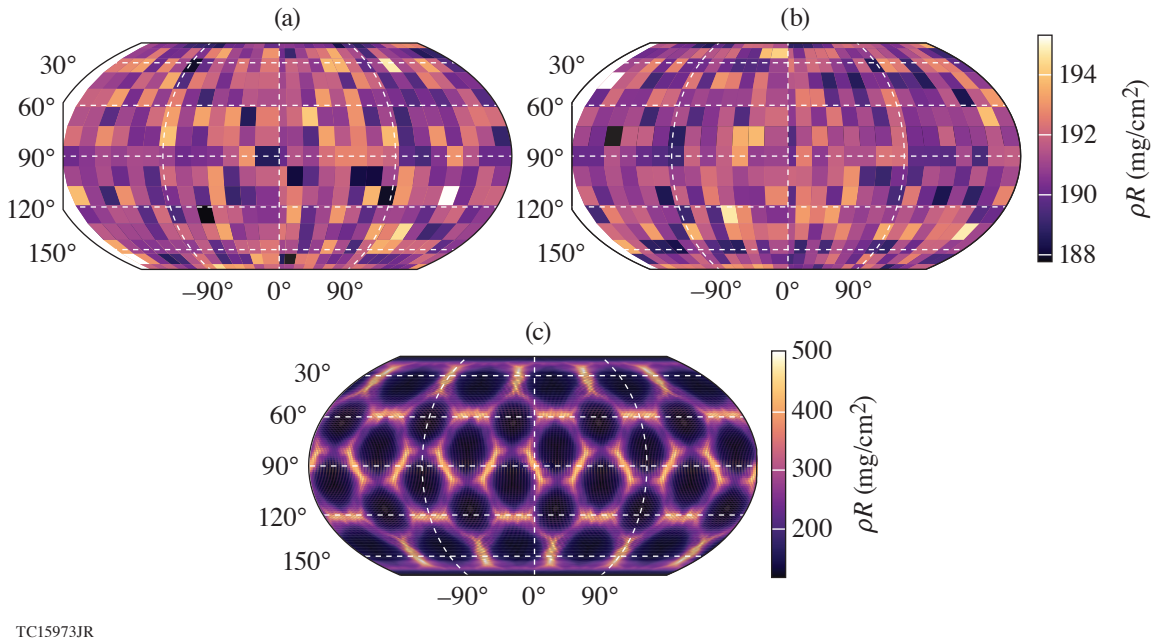

Figure 1
A projection of (a) the inferred ρR from the backscatter edge, (b) the inferred ρR from the forward-scatter edge for a simulation, and (c) $\int \rho dr$ at bang time for a simulation with a target of radius 490 μm and a laser beam with radius 330 μm. Despite a rather large perturbation being driven, the effects of distributed source and integration over the edge result in no observable structured variation.

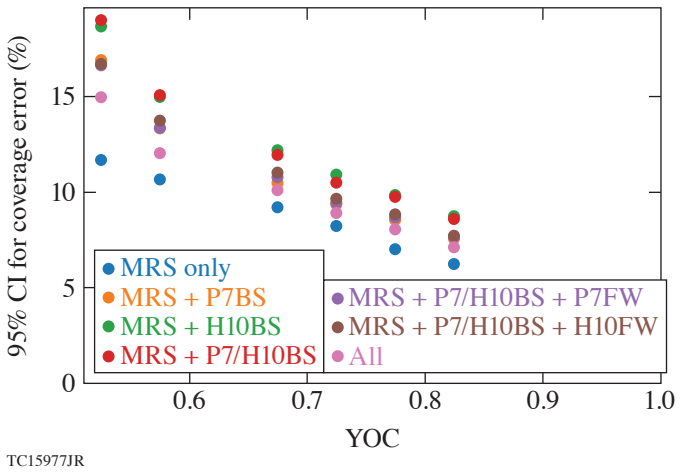

Figure 2
The 2σ upper bound on the coverage error for each detector permutation for simulations with similar yield over clean (YOC), over a range of YOC's. Unlike with the $\ell = 1$ case, there is no observable parameterizing the degradation due to $\ell = 2$, and so the YOC is used directly. Unlike the $\ell = 1$ case, adding any one backscatter detector increases the error rather than decreasing it. Although the addition of the forward-scatter measurements on the nTOF's does decrease the error relative in the case where only backscatter nTOF measurements are considered, they nevertheless are not reduced below the level when only the MRS is considered. Since this is a result of the relative orientations of the nTOF and MRS detectors on OMEGA, this is a result specific to the OMEGA setup, and not a general observation. CI: confidence interval.

In the $\ell = 2$ mode case, the strength of the mode is parametrized by its yield degradation YOC = $Y_{3\text{-D}}/Y_{1\text{-D}}$, and bin the various configurations accordingly, as before. The results are visualized in Fig. 3. First, using only the MRS forward-scatter measurement results in a lower error than combining the MRS with any backscatter measurement. This counterintuitive result can be understood when the relative orientations of various integration regions are considered. In the $\ell = 1$ case considered above, the orientations meant that the H10 backscatter measurement was strongly anticorrelated with the MRS (since the ρR varied with an $\ell = 1$ pattern), while the P7 backscatter measurement was only weakly correlated with the MRS. Since the $\langle \rho R \rangle$ lies in between the maxima and minima, an average (by whatever mechanism) of measurements best reproduces the $\langle \rho R \rangle$ if some measurements are greater than $\langle \rho R \rangle$, and some are less. In the $\ell = 2$ case, H10 and P7 backscatter measurements are, due to their specific orientations on the

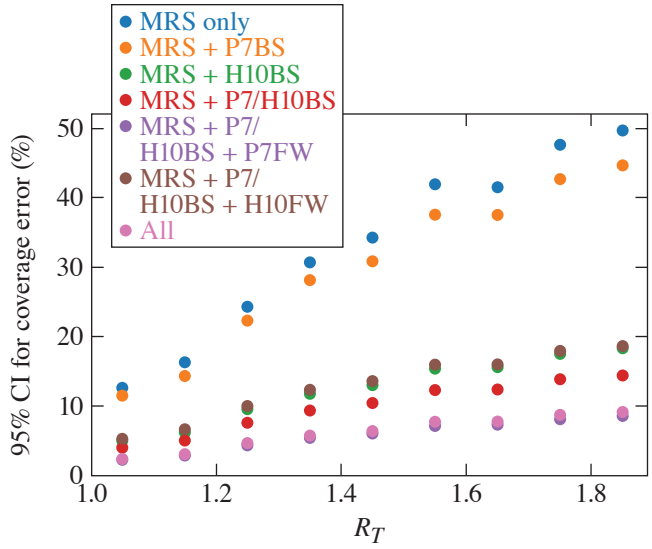

Figure 3
The 2σ upper bound on the coverage error for each detector permutation for all simulations with similar R_T over a range of R_T. First, note that having only the MRS (blue circles) has an extremely high error for even small values of R_T. Adding the P7 nTOF (orange circles) is not as valuable as adding the H10 nTOF (green circles) since the P7 backscatter and MRS forward-scatter regions are nearer to each other than the H10 backscatter and MRS forward scatter, and vice versa for the hypothetical P7 and H10 forward-scatter measurement. Nevertheless, adding all five detector configurations significantly reduces error from the currently used detector configuration.

OMEGA system, well correlated with the MRS (H10 more so than P7). In addition, the backscatter measurements sample a much smaller region of the shell than the forward scatter and, thus, have a higher probability of measuring an extremely different ρR from the MRS (again, H10 more than P7). Therefore, when including them in an average, it is possible to move the average further away from the $\langle \rho R \rangle$, and thereby increase the composite error. From there, including additional forward-scatter measurements either from P7 or H10 detectors reduces the error since a larger region of the shell is sampled. However, it is insufficient to correct for the bias induced by the backscatter measurement.

Finally, having established a measure of the likely values of how the measured ρR deviates from $\langle \rho R \rangle$ that can be expected under reasonable conditions, one considers whether it is possible to recover $\langle \rho R \rangle$, even if only in restricted cases. Here, the only case considered will be where the $\ell = 1$ mode dominates. The reason for choosing only this case is that the $\ell = 1$ case is the only one where the yield degradation due to the mode can be inferred on OMEGA at this time. Defining $R_{\rho R} = \rho R / \langle \rho R \rangle$ as the deviation of the measured ρR at some line of sight from the true 4π average $\langle \rho R \rangle$, it is noted that since the orientation of the mode with respect to each detector is known and deterministic, it is reasonable to presume that there ought to be a relationship between the $R_{\rho R}$ at the detector location and both a measure of the mode amplitude and the central angle y between the mode maximum and detector position. The mode amplitude can be parametrized either by the R_T, or by the ratio of the bulk flow to the implosion velocity $\tilde{v}$. A suggested ansatz for $R_{\rho R}$ is given by

$$R_{\rho R} \cdot (R_T, \psi) = R_T \alpha + A(R_T - 1)\beta \cos(\psi - \psi_0), \tag{2}$$

$$R_{\rho R} \cdot (\tilde{v}, \psi) = \exp(\alpha \tilde{v}) + A\tilde{v}\beta \cos(\psi - \psi_0), \tag{3}$$

where A, α, β, and ψ_0 are constants that differ for forward and backward scatter and will be determined by fitting to the data, and are summarized in Table III. A graphic presentation the quality of the fits is shown in Fig. 4 and indicates that Eqs. (2) and (3) accurately represent the modulation of ρR over the sphere.

Using the coefficients in Table I, it is also possible to calculate a final "prediction" of the ρR that would be used in experiments, assuming only the existing OMEGA detectors are used. This is shown in Fig. 5, where the arithmetic average of the detector predictions using the coefficients in Table III is shown for each simulation in the $\ell = 1$ dataset. If such a reconstruction could be performed on OMEGA, the uncertainty from the $\ell = 1$ modes can be made sufficiently low (<3.5%) for incremental iterative schemes to be successful on OMEGA. This suggests that generating such procedures for $\ell = 2$ should be a high priority since these modes are known to exist on OMEGA.

Table III: Fit parameters of Eqs. (2) and (3) for the forward and backscatter detectors.

Detector	α	β	ψ	A
Forward scatter (R_T)	0.34	0.62	–0.21	0.65
Backscatter (R_T)	0.46	0.64	–0.24	–0.78
Forward scatter ($\tilde{v}$)	0.32	1.09	–0.24	1.07
Backscatter ($\tilde{v}$)	0.44	1.05	0.37	–1.22

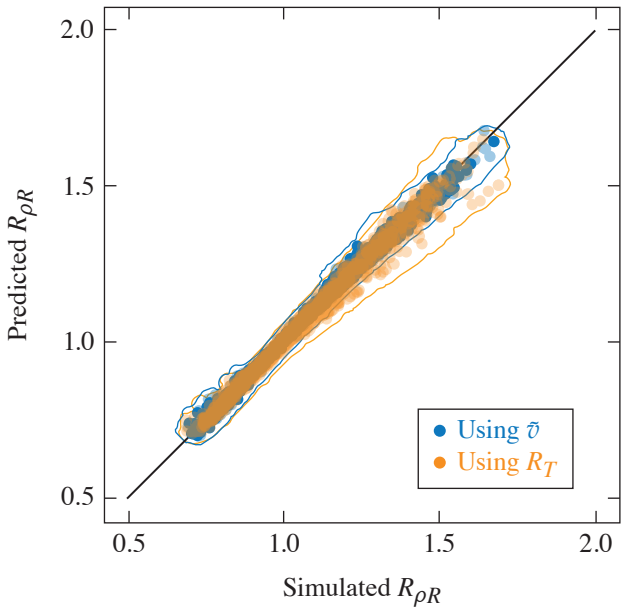

TC15980JR

Figure 4
The accuracy of Eq. (2) (orange circles) and Eq. (3) (blue circles) in reconstructing the $R_{\rho R}$ across the entire dataset for each detector separately, assuming the orientation and amplitude of the $\ell = 1$ mode is known. Due to the large number of points in the full dataset, 10% are selected randomly and plotted. The solid line shows the extent of the full dataset for both cases. The $R_{\rho R}$ calculated from the simulations is on the horizontal axis, while the prediction from Eqs. (2) and (3) is on the vertical axis.

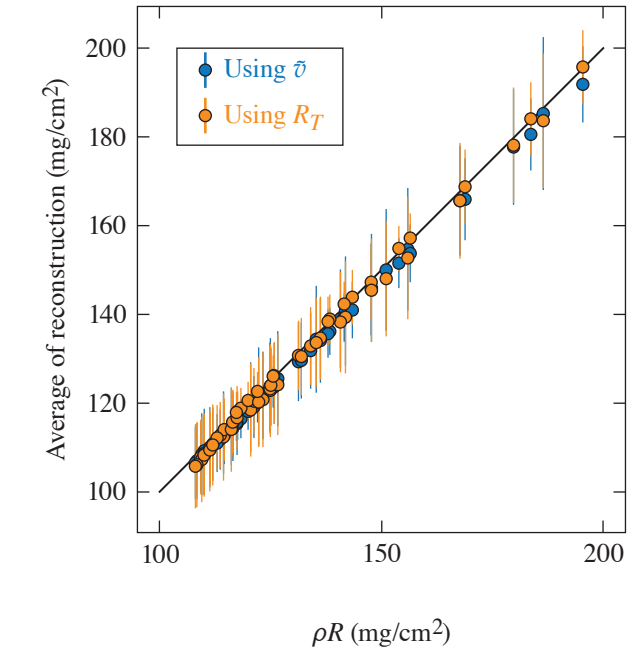

TC15981J1

Figure 5
The accuracy of harmonically averaging the reconstructed ρR inferred using Eq. (2) (blue circles) and Eq. (3) (orange circles) in predicting $\langle \rho R \rangle$ for all simulations in the dataset using only the MRS and P7/H10 backscatter detectors, assuming the orientation and amplitude of the $\ell = 1$ mode is known. Error bars represent the 2σ range of the reconstruction when varying mode orientations with respect to fixed detector locations. The method is clearly accurate across the full range of conditions, with an rms error of roughly 3.5% for both the R_T and ($\tilde{v}$) models.

Accurate measurements of the ρR are integral to an accurate understanding of the performance of cryogenic direct-drive ICF experiments on OMEGA. Quantifying and rectifying the errors that are incurred by incomplete coverage are a necessary step toward achieving the accuracy necessary to design OMEGA experiments that will scale to hydrodynamically equivalent ignition. Quantifying this error is also a step toward a quantification of the total uncertainty in the 1-D–equivalent ρR that arises as a combination of coverage and measurement uncertainty. Considered here are the effects of limited detector coverage over a range of core conditions using *ASTER* simulations, post-processed with *IRIS* with varying $\ell = 1$ and 2 modes, for a number of permutations of existing and hypothetical detectors used on OMEGA. The expected uncertainty is quantified due to the induced asymmetry over the credible range of expected perturbations on OMEGA. It is then found that the error due to limited detector coverage tends to decrease as additional detectors are added in the $\ell = 1$ case, but find that due to the specific detector geometry on OMEGA, the $\ell = 2$ coverage uncertainty can increase as additional backscatter measurements are made. The coverage error due to the $\ell = 1$ mode is robustly eliminated if the existing nTOF detectors on OMEGA were capable of forward-scattering measurements. After postulating that the orientation and yield degradation caused by a mode could be used to reconstruct the 1-D–equivalent ρR, it is shown that this is indeed possible in cases that are dominated by large $\ell = 1$ modes, and that the error in reconstructing the true 1-D–equivalent ρR can be made acceptably low with existing OMEGA diagnostics.

This material is based upon work supported by the Department of Energy National Nuclear Security Administration under Award Number DE-NA0003856, the University of Rochester, and the New York State Energy Research and Development Authority.

1. J. D. Lawson, Proc. Phys. Soc. Lond. B **70**, 6 (1957).
2. R. Betti and O. A. Hurricane, Nat. Phys. **12**, 435 (2016).
3. A. R. Christopherson *et al.*, Phys. Plasmas **25**, 012703 (2018).
4. R. Betti *et al.*, Phys. Plasmas **17**, 058102 (2010).
5. P. Y. Chang *et al.*, Phys. Rev. Lett. **104**, 135002 (2010).
6. B. K. Spears *et al.*, Phys. Plasmas **19**, 056316 (2012).
7. R. Betti *et al.*, Phys. Rev. Lett. **114**, 255003 (2015).
8. C. D. Zhou and R. Betti, Phys. Plasmas **14**, 072703 (2007).
9. T. R. Boehly *et al.*, Opt. Commun. **133**, 495 (1997).
10. V. Gopalaswamy *et al.*, Nature **565**, 581 (2019).
11. A. Lees *et al.*, Phys. Rev. Lett. **127**, 105001 (2021).
12. V. Gopalaswamy *et al.*, Phys. Plasmas **28**, 122705 (2021).
13. I. V. Igumenshchev *et al.*, Phys. Plasmas **23**, 052702 (2016).
14. M. Gatu Johnson *et al.*, Rev. Sci. Instrum. **89**, 10I129 (2018).
15. C. J. Forrest *et al.*, Rev. Sci. Instrum. **83**, 10D919 (2012).